Journal of Sound and Vibration (2002) **256**(4), 629–645
doi:10.1006/jsvi.5012, available online at http://www.idealibrary.com on IDEAL®

VIBRATION SUPPRESSION OF A BEAM STRUCTURE BY INTERMEDIATE MASSES AND SPRINGS

K. ALSAIF AND M. A. FODA

Department of Mechanical Engineering, King Saud University, P.O. Box 800, *Riyadh* 11421, *Saudi Arabia. E-mail*: *mfoda@ksu.ed.sa*

(*Received* 28 *February* 2001, *and in final form* 17 *September* 2001)

A method based on the dynamic Green function has been proposed to determine the optimum values of masses and/or springs and their locations on a beam structure in order to confine the vibration at an arbitrary location. In the analysis, the beam is driven by a harmonic external excitation. The added masses on the beam and the springs attached are modelled as simple reactions that provide transverse forces to the beam. These forces act as secondary forces that reduce the response caused by the external force. Numerical simulation shows that the vibration of the beam can be confined in a certain region by the presence of masses and springs in best arrangement. This method is demonstrated for both a simply supported and a cantilever beam. An experimental set-up was designed in which a simply supported beam is excited by an electrodynamic shaker and the response of the beam is measured using an He–Ne laser system. This assures very accurate measurements and avoids any additional loading effects as in the case of accelerometers. Comparisons of the theoretical and the experimental results show good agreement.

1. INTRODUCTION

Many components in a mechanical system can be modelled as beams subjected to disturbances resulting in a vibratory motion. If these beams are flexible and have low inherent damping, the vibratory motion can last for a long time before it dies out. This creates problems in the structural performance of these members. Vibrational confinement and control has evolved in order to improve structural performance. The ideas suggested range from the use of passive control (utilizing added masses, springs, dampers, etc.) to the use of active control with sophisticated control strategies (utilizing sensors, actuators, feedback etc.).

In recent years, much attention has been placed on the vibrational confinement and control of flexible structures. In certain applications, it may be of interest to eliminate vibration from one part of the structure more than another. Large flexible space structures, for example, are usually built from lightweight materials with low damping, and will be very flexible due to the thin large-size elements from which they are constructed. An excitation source may cause vibrations that propagate throughout the structure. In such a case, it is desirable to confine vibration in some chosen insensitive part while keeping other parts, for instance an extremely sensitive antenna, relatively unaffected.

The purpose of this paper is to investigate the effect of added masses and/or springs on beam vibration. A technique based on the dynamic Green function is developed to give the best arrangement of masses and/or springs, for vibration confinement in a certain part of a sinusoidally driven beam. The optimum mass ratio is obtained at each external exciting

0022-460X/02/$35.00

frequency. The effect of the input force on the magnitude of the suppressed vibration amplitude is also investigated. Some of the objectives of the present work are similar to those of Keltie and Cheng [1] who used a modal analysis approach to investigate the effects of added masses on vibrational behavior of a simply supported beam and furthermore utilized the results to control or reduce the vibration response. In their optimization techniques, they considered only the mass locations as design parameters. Furthermore, the vibration suppression region considered in their study was either on the left side or the right side of the beam; no attempt was made to investigate the vibration reduction within intermediate regions along the beam. In the present paper, a single mass or a spring is attached to the beam at a prescribed location to maintain a significantly small vibration level at a particular location along the beam.

The determination of the natural frequencies and mode shapes of restrained beams with springs and point masses attached has been investigated by many authors for various beam boundary conditions [2–8]. In these references, numerical approaches such as the transfer matrix method, finite element method, analytical and numerical combined method as well as pure analytical (closed form) solutions for a few special cases are adopted. For any kind of boundary conditions, the exact natural frequencies and mode shapes for a beam with attached point masses and/or springs can be obtained as a result of the present analysis.

Formulation of the solution for the present problem is done by utilizing the Green functions. This method is exact, direct, short and elegant. This procedure was chosen for its freedom from numerical inaccuracy when compared to standard application of modal series techniques. Equally important, this procedure exhibits appreciably greater computational efficiency when compared with the modal analysis approach. Therefore, it can be used by any engineer of a pragmatical nature without any difficulty.

2. FORMULATION

The problem to be considered is that of transverse vibration of a uniform elastic beam of finite length L originally at rest with different classical or unconventional boundary conditions at $x = 0$ and L, not shown in Figure 1. The beam is driven by a sinusoidal external force and there are R point masses and N springs attached to the beam. The lateral vibration of the beam is governed by the equation

$$EI\,\frac{\partial^4 w(x,t)}{\partial t^4} + \rho A\,\frac{\partial^2 w}{\partial t^2} = -\sum_{r=1}^{R} m_r\,\frac{\partial^2 w(x,t)}{\partial t^2}\,\delta(x-b_r) - \sum_{i=1}^{N} K_i w(x,t)\,\delta(x-a_i) + f_{ext}, \tag{1}$$

where EI, ρ, A, and $w(x, t)$ denote, respectively, the flexural rigidity of the beam, the density, the cross-sectional area, and the transverse deflection of the beam at point x and at time t. b_r represents the location of the rth mass m_r while a_i represents the location of the ith spring K_i.

The external force f_{ext} is given as

$$f_{ext} = F_0\,\mathrm{e}^{\mathrm{j}\omega t}\,\delta(x-x_0), \tag{2}$$

where ω and x_0 are the force frequency and force location, respectively, and $\delta(\cdot)$ is the Dirac delta function.

The solution of equation (1) is assumed to be harmonic in time, thus

$$w(x,t) = W(x)\,\mathrm{e}^{\mathrm{i}\omega t}, \tag{3}$$

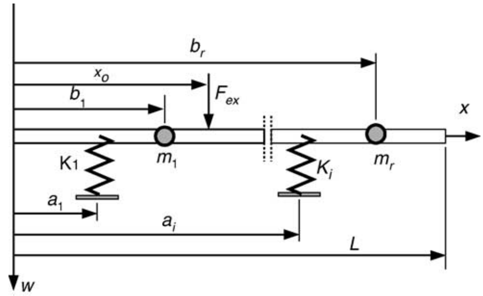

Figure 1. A uniform beam with attached point masses and springs.

and this reduces equation (1) to

$$\frac{\mathrm{d}^4 W(x)}{\mathrm{d}x^4} - q^4 W(x) = \frac{1}{EI}\left\{\sum_{r=1}^{R} m_r \omega^2 W(x)\,\delta(x-b_r) - \sum_{i=1}^{N} K_i W(x)\,\delta(x-a_i) + F_0\,\delta(x-x_0)\right\}, \quad (4)$$

where

$$q^4 = \rho A \omega^2 / EI. \quad (5)$$

The dynamic Green function is utilized to find the solution for equation (4). Hence if G(x, u) is the dynamic Green function, as yet unknown, for the stated problem, then the solution of equation (3) takes the form

$$w(x,t) = \frac{1}{EI}\int_0^L \sum_{r=1}^{R} m_r\,\omega^2 W(u)\,\mathrm{G}(x,u)\,\delta(u-b_r)\mathrm{d}u - \frac{1}{EI}\int_0^L \sum_{i=1}^{N} K_i\,W(u)\,\mathrm{G}(x,u)\,\delta(u-a_i)\mathrm{d}u + \frac{1}{EI}F_0\int_0^L \mathrm{G}(x,u)\,\delta(u-x_0)\,\mathrm{d}u. \quad (6)$$

Performing the integration one obtains

$$W(x) = \frac{\omega^2}{EI}\sum_{r=1}^{R} m_r\,W(b_r)\,\mathrm{G}(x,b_r) - \frac{1}{EI}\sum_{i=1}^{N} K_i\,W(a_i)\,\mathrm{G}(x,a_i) + \frac{F_0}{EI}\mathrm{G}(x,x_o), \quad (7)$$

where G(x, u) is the solution of the differential equation

$$\mathrm{d}^4/\mathrm{d}x^4\,\mathrm{G}(x,u) - q^4\,\mathrm{G}(x,u) = \delta(x-u) \quad (8)$$

The solution of equation (8) is assumed in the form reported in reference [9].

$$\mathrm{G}(x,u) = \begin{Bmatrix} A_1\cosh(qx) + A_2\sinh(qx) + A_3\cos(qx) + A_4\sin(qx), & 0 \leqslant x \leqslant u \\ \bar{A}_1\cosh(qx) + \bar{A}_2\sinh(qx) + \bar{A}_3\cos(qx) + \bar{A}_4\sin(qx), & x \leqslant u \leqslant L \end{Bmatrix}, \quad (9)$$

The eight constants $A_1, \ldots, A_4$ and $\bar{A}_1, \ldots, \bar{A}_4$ are evaluated such that the Green function G(x, u) satisfies the following conditions [10]: (1) two boundary conditions at each end of the beam depending on the type of end support; (2) transient conditions, namely continuity conditions of displacement, slope and moment at $x = u$, i.e.,

$$G(x, u)|_{x=u^+} = G(x, u)|_{x=u^-}, \qquad dG(x, u)/dx|_{x=u^+} = dG(x, u)/dx|_{x=u^-},$$

$$d^2G(x, u)/dx^2|_{x=u^+} = d^2G(x, u)/dx^2|_{x=u^-}; \tag{10}$$

(c) shear force discontinuity of magnitude one at $x = u$, i.e.,

$$d^3G(x, u)/dx^3|_{x=u^+} - d^3G(x, u)/dx^3|_{x=u^-} = 1. \tag{11}$$

For a simply supported beam, the Green function as determined by the above procedure is given by

$$G(x, u) = \frac{1}{2q^3 \sin(qL)\sinh(qL)} \begin{cases} g(x, u), & 0 \leqslant x \leqslant u \\ g(u, x), & x \leqslant u \leqslant L \end{cases}, \tag{12}$$

where

$$g(x, u) = \sinh(qL)\sin(qx)\sin(qL - qu) - \sin(qL)\sinh(qx)\sinh(qL - qu) \tag{13}$$

and $g(u, x)$ is obtained by switching x and u in $g(x, u)$. This follows from the fact that $G(x, u)$ must be symmetric to satisfy the Maxwell–Rayleigh reciprocity law.

To this end, one evaluates the $W(x)$ from equation (7) at all points of spring and mass attachments, i.e., at $x = a_i$ and $x = b_r$, for $i = 1$–N and $r = 1$–R. This gives $N + R$ equations with $N + R$ unknowns being:

$$\tilde{W}(a_1), \tilde{W}(a_2), \ldots, \tilde{W}(a_N), \tilde{W}(b_1), \tilde{W}(b_2), \ldots, \tilde{W}(b_R).$$

These equations can be written concisely in matrix form

$$[\mathbf{D}]\{\tilde{\mathbf{W}}\} = \{\mathbf{C}\}, \tag{14}$$

where

$$\{\tilde{W}\} = \{W(a_1), W(a_2), \ldots, W(a_N), W(b_1), W(b_2), \ldots, W(b_R)\}^T, \tag{15}$$

$$\{\mathbf{C}\} = \alpha\{G(a_1, x_0), G(a_2, x_0), \ldots, G(a_N, x_0), G(b_1, x_0), G(b_2, x_0), \ldots, G(b_R, x_0)\}^T \tag{16}$$

and the matrix $D = [I] + [B]$, where $[I]$ is the identity matrix and the matrix $[B]$ is

$$[B] = [\gamma_1\{\mathbf{u}_1\}, \ldots, \gamma_i\{\mathbf{u}_i\}, \ldots, \gamma_N\{\mathbf{u}_N\}\beta_1\{\mathbf{V}_1\}, \ldots, \beta_r\{\mathbf{V}_r\}, \ldots, \beta_R\{\mathbf{V}_R\}], \tag{17}$$

where

$$\{\mathbf{u}_i\} = \{G(a_1, a_i), G(a_2, a_i), \ldots, G(a_N, a_i), G(b_1, a_i), G(b_2, a_i), \ldots, G(b_R, a_i)\}^T, \tag{18}$$

$$\{\mathbf{V}_r\} = \{G(a_1, b_r), G(a_2, b_r), \ldots, G(a_N, b_r), G(b_1, b_r), G(b_2, b_r), \ldots, G(b_R, b_r)\}^T \tag{19}$$

TABLE 1

Experimental model parameters

Beam length (m)	Width (m)	Thickness (m)	Density (kg/m^3)	Young's modulus (N/m^2)
0·75	0·03	0·003	7700	$19{\cdot}5 \times 10$

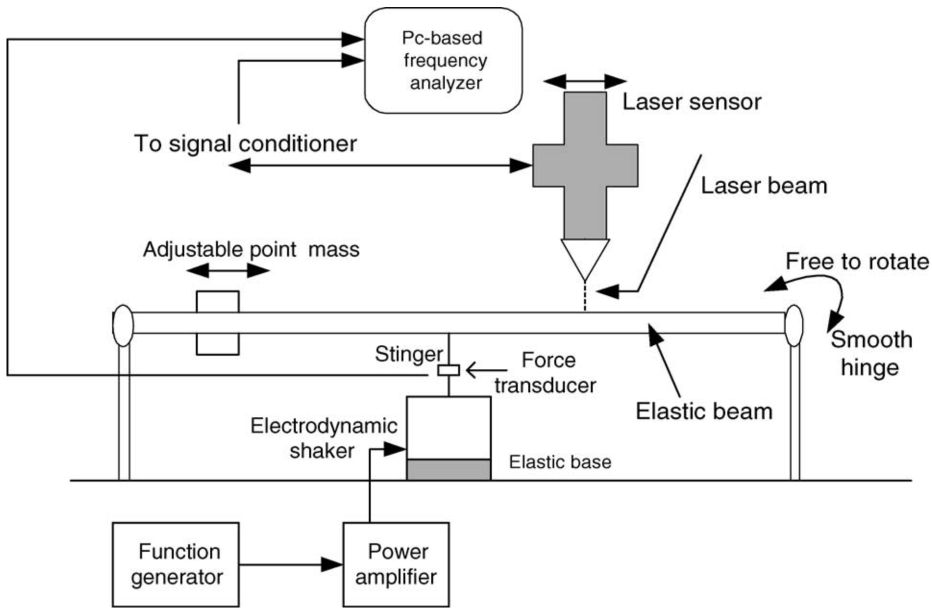

Figure 2. Experimental set-up.

and

$$\gamma_i = K_i/EI, \qquad \beta_r = -\,\omega^2 m_r/EI, \qquad \alpha = F_0/EI. \tag{20}$$

The unknown displacement vector $\{\tilde{\mathbf{W}}\}$ can be obtained by solving the matrix equation (14). One next substitutes the displacement vector $\{\tilde{\mathbf{W}}\}$into equation (7) to obtain the deflection at any point x in the beam. Specifically,

$$W(x) = -\sum_{i=1}^{N} \gamma_i W(a_i)\,\mathrm{G}(x, a_i) - \sum_{r=1}^{R} \beta_r\, W(b_r)\,\mathrm{G}(x, b_r) + \alpha \mathrm{G}(x, x_0). \tag{21}$$

It is worth observing that if one is interested in evaluating the natural frequencies of the beam with mass and/or spring attachments, the determinant of the matrix $[\mathbf{D}]$ can be set equal to zero to obtain a highly non-linear frequency equation involving transcendental functions which can be solved by appropriate techniques.

3. EXPERIMENTAL SET-UP

In order to verify the analytical results, a set of experiments was conducted for the case of a simply supported beam with adjustable point masses that can slide along the beam. The system parameters and material properties are listed in Table 1. Figure 2 shows the

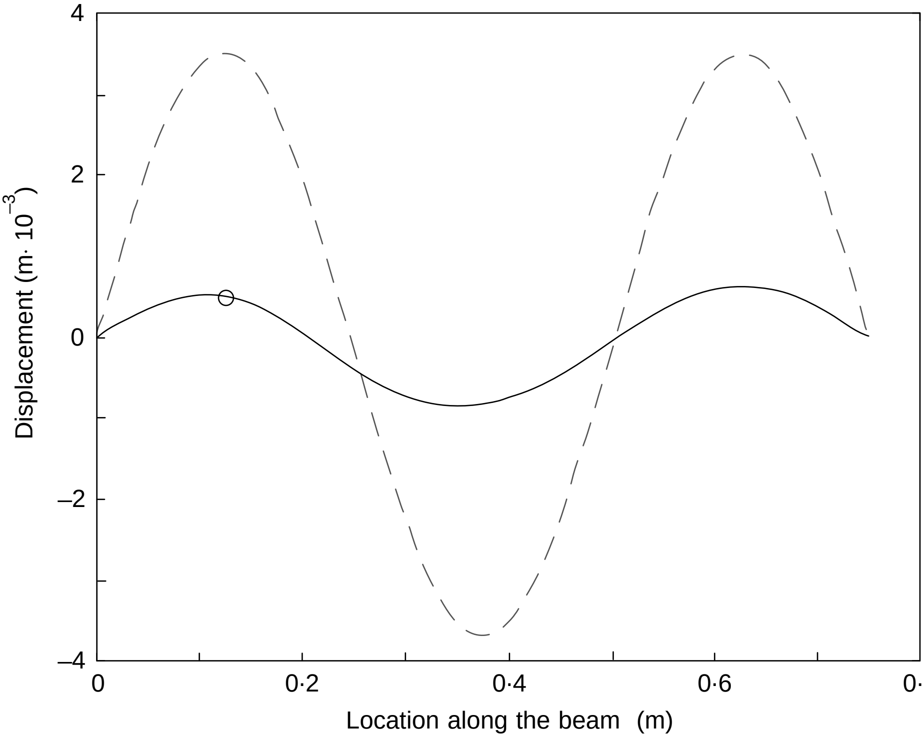

Figure 3. Analytical displacement responses of the loaded and unloaded simply supported beam when $\omega = 112$ Hz, $F_0 = 20$ N, $m_1 = 0{\cdot}065$ kg at $b_1 = 0{\cdot}1236$ m. ------, Unloaded; ——, loaded; ○, mass location.

experimental set-up used in the experiment. The beam is loaded with a single mass of 0·065 kg located at $x = 0{\cdot}1236$ m as shown. The electrodynamic shaker provides a harmonic input force to the beam at its mid-span. The force amplitude is kept constant at 20 N and the frequency is varied. The steady state displacement response is measured at several points along the beam using a laser transducer. A laser beam reflector is attached at the points of measurement and the reflected signal is processed and connected to a frequency analyzer. Unlike accelerometers, using a laser sensor, the mass-loading effect is eliminated. It should mentioned that displacement measurements in the neighborhood of 10-μm can be made.

4. VERIFICATION OF THE MATHEMATICAL MODEL

Consider the simply supported beam described in the previous section. The analytical solution of the dynamic displacement of the beam with an attached mass, 0·065 kg, at location $x = 0{\cdot}25\,\lambda$ (0·1236 m) with an input excitation frequency $\omega = 112$ Hz can be obtained from equation (21). The spatial wavelength of the flexural wave is $\lambda = 2\pi/k_b$, where $k_b = q^{1/4}$ is the wavenumber. Using Matlab software, the displacement response of the beam is depicted in Figure 3. The figure shows the response of the mass-loaded and the unloaded beam. Figures 4 and 5 show the comparison between the numerical and experimental steady state response of the mass-loaded and unloaded beam respectively. The figures indicate a good match between the two results. Therefore, the analytical model reproduces the experimental results with acceptable accuracy.

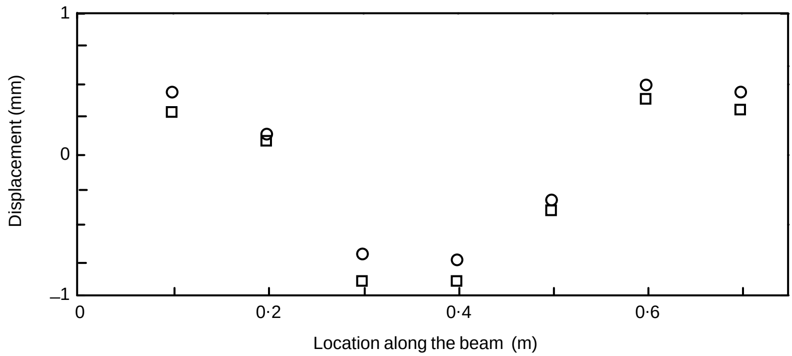

Figure 4. Comparison between experimental and analytical displacement responses of the loaded simply supported beam when $\omega = 112$ Hz, $F_0 = 20$ N, $x_0 = L/2$, $m_1 = 0{\cdot}065$ kg. ○, Analytical; □, experimental.

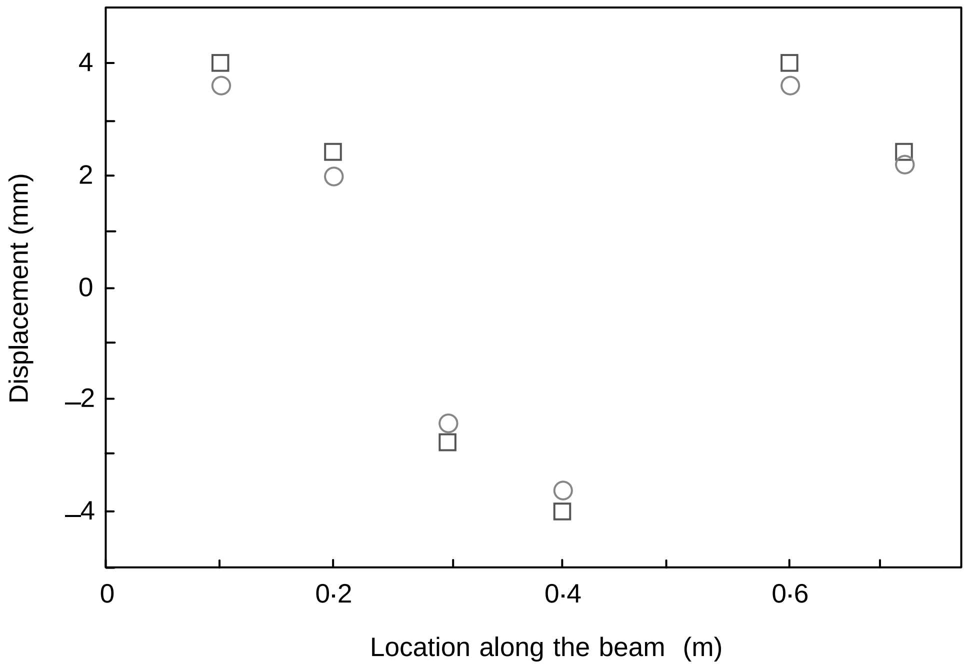

Figure 5. Comparison between experimental and analytical displacement responses of the unloaded simply supported beam when $\omega = 112$ Hz, $F_0 = 20$ N, $x_0 = L/2$. ○, Analytical; □, experimental.

5. PARAMETRIC STUDY

With the confidence gained from the comparison between Figures 4 and 5, a parametric study using the developed analytical model has been conducted. Simply supported as well as cantilevered beams are considered. The parameters selected for the simply supported beam in the numerical simulations correspond to the data used in reference [1]. The beam span $L = 20$ m, modulus of elasticity $E = 19{\cdot}5 \times 10^{10}$ N/m^2, thickness h $= 0{\cdot}026458$ m, width $b = 1$ m, and density $\rho = 7700$ kg/m^3. Therefore, the mass of the beam $m_b = 4073$ kg. In all the figures, the dashed lines represent the transverse displacement of the unloaded beam (beam without attachments).

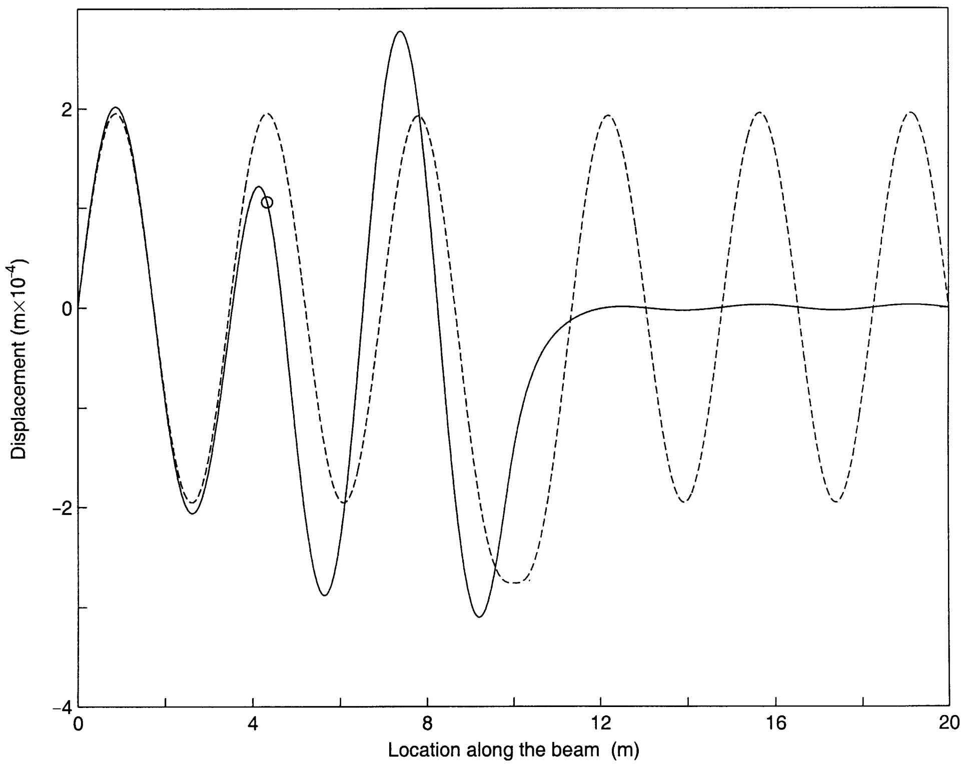

Figure 6. Analytical displacement responses of the loaded and unloaded simply supported beam when $\omega = 20$ Hz, $F_0 = 1000$ N, $x_0 = 10$ m, $m_1 = 410$ kg at $b_1 = 4{\cdot}3436$ m. ——, Loaded; ------, unloaded; ○, mass location.

Figure 6 shows the dynamic response of the beam for a relatively low excitation frequency $\omega = 20$ Hz (compared to the fundamental natural frequency of the beam). The excitation force amplitude $F_0 = 1000$ N acts at the mid-span of the beam; $x_0 = 10$ m. It is observed that the smallest mass suppressing the vibration in the right half of the beam should be attached in the left half at any peak or trough of the flexural displacement of the unloaded beam. In the figure, a single mass of 410 kg is attached at $b_1 = 4{\cdot}3436$ m which corresponds to 1·25 λ. If one is interested in controlling the vibration in the left half of the beam, a mass of the same value should be attached in the right half instead as shown in Figure 7. It should be noted that two equal masses, of 140 kg each can be attached at any two peaks or troughs (or combination) of the flexural wave of the unloaded beam to give exactly the same effect of a single mass.

To address the physical explanation of the behavior observed, one returns to the investigation of the effect of the added mass. The added mass was treated as purely inertial reaction acting as a control force (secondary force) with a magnitude dependant upon the square of the driving frequency, the displacement amplitude at its location and the value of the mass. Specifically, $F_i = m\omega^2 W(b_1)$. This secondary force creates a flexural wave that is out of phase of the flexural wave generated by the external force (the primary force). As a result, the sum of the two waves is zero at one side of the excitation force. This is depicted in Figure 8. The dashed–dot–dashed line represents the flexural wave due to the added mass given in Figure 6. This added mass corresponds to an inertial force $\mathrm{F}_i = 685{\cdot}0118$ N acting at location 4·3436 m. The dashed line represents the flexural wave due to the primary force

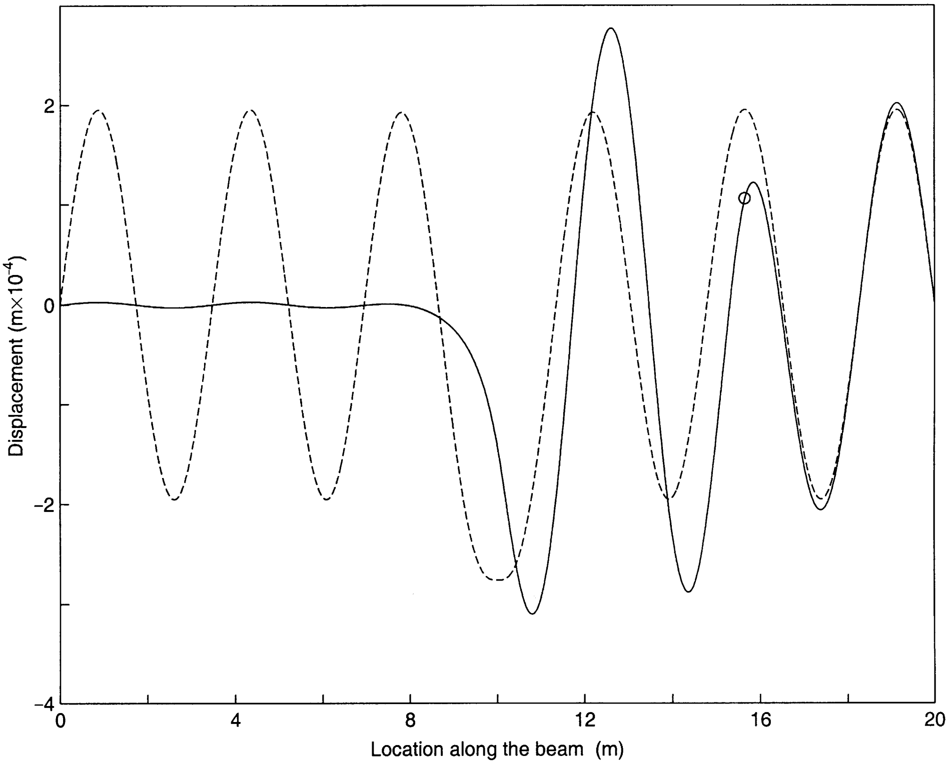

Figure 7. Analytical displacement responses of the loaded and unloaded simply supported beam when $\omega = 20$ Hz, $F_0 = 1000$ N, $x_0 = 10$ m, $m_1 = 410$ kg at $b_1 = 15{\cdot}6564$ m. ——, Loaded; ------, unloaded; ○, mass location.

$F_0 = 1000$ N acting at $x_0 = 10$ m. These two waves are 180° out of phase in the right half of the beam. Therefore, the mixing of the two waves results in destructive interference. Comparable phenomena are encountered in noise cancellation by introducing opposing sound sources [11].

Figure 9 depicts the dynamic response of the beam for intermediate frequency excitation $\omega = 60$ Hz. The excitation force acts at mid-span with an amplitude $F_0 = 1000$ N. A single mass of value 13·5 kg is attached at 8·525 m; which, corresponding to 4·25 λ, is needed to suppress the vibration in the right half of the beam. Instead one can use two masses each of 6·5 kg, or a set consisting of three masses of 4·33 kg each. Alternatively, a set consisting of four masses each equals 3·25 kg can be used. In all these alternative choices, masses are attached in the left half of the beam at peaks or troughs of the flexural wave of the unloaded beam.

In Figure 10, the excitation frequency is relatively high, $\omega = 100$ Hz. The excitation force acts at the mid-span of the beam with an amplitude of 1000 N. One needs to attach a 55·5 kg mass at the left half to cancel the vibration in the right half of the beam. With regards to the change of the location of the excitation force, Figure 11 indicates the transverse displacements when the force acts at $x_0 = 6$ m. For the unloaded beam, the vibrational amplitude to the right of the force is more pronounced than that to the left of the force. However, the attachment of 299 kg mass can shift all the vibrational energy to the left of the force and leave the right region at rest position. The added mass appears to be relatively large; however the mass ratio is 0·0734 which is acceptable for engineering applications. Another interesting observation is that a similar effect can be obtained by using a spring

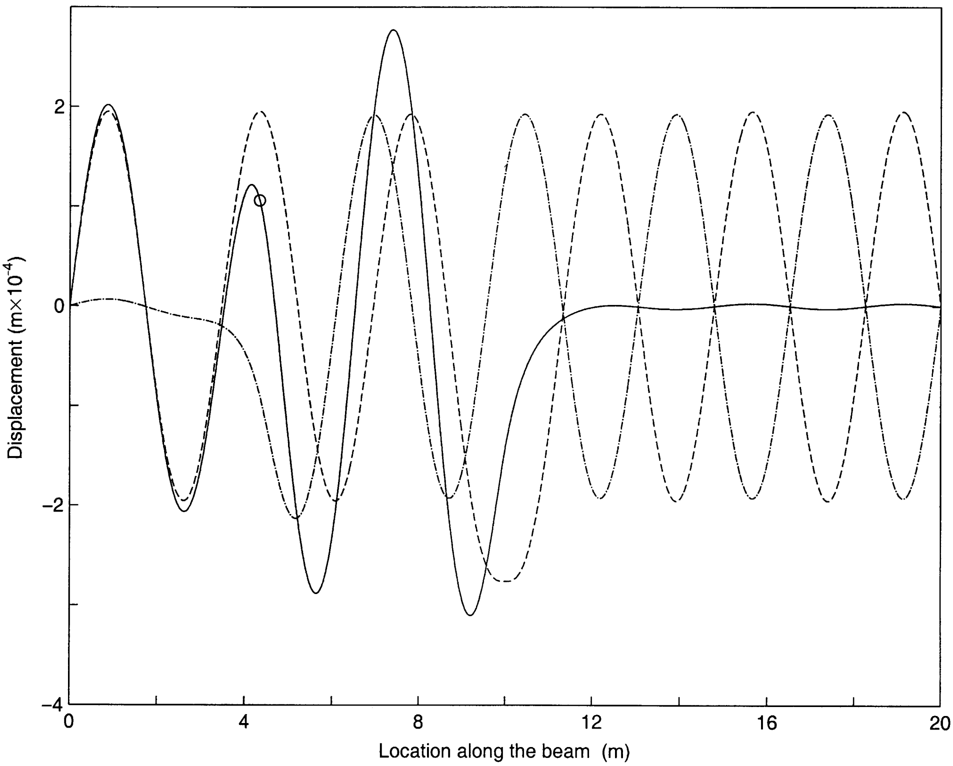

Figure 8. Analytical displacement responses of the loaded and unloaded simply supported beam when $\omega = 20$ Hz. ------, Unloaded with $F_0 = 1000$ N, $x_0 = 10$ m, –·–·–, unloaded; with $F_i = 685{\cdot}0118$ N, $x_i = 4{\cdot}3436$ m; ——, loaded with $F_0 = 1000$ N, $x_0 = 10$ m, $m = 410$ kg at $b_1 = 15{\cdot}6564$ m; ○, mass location.

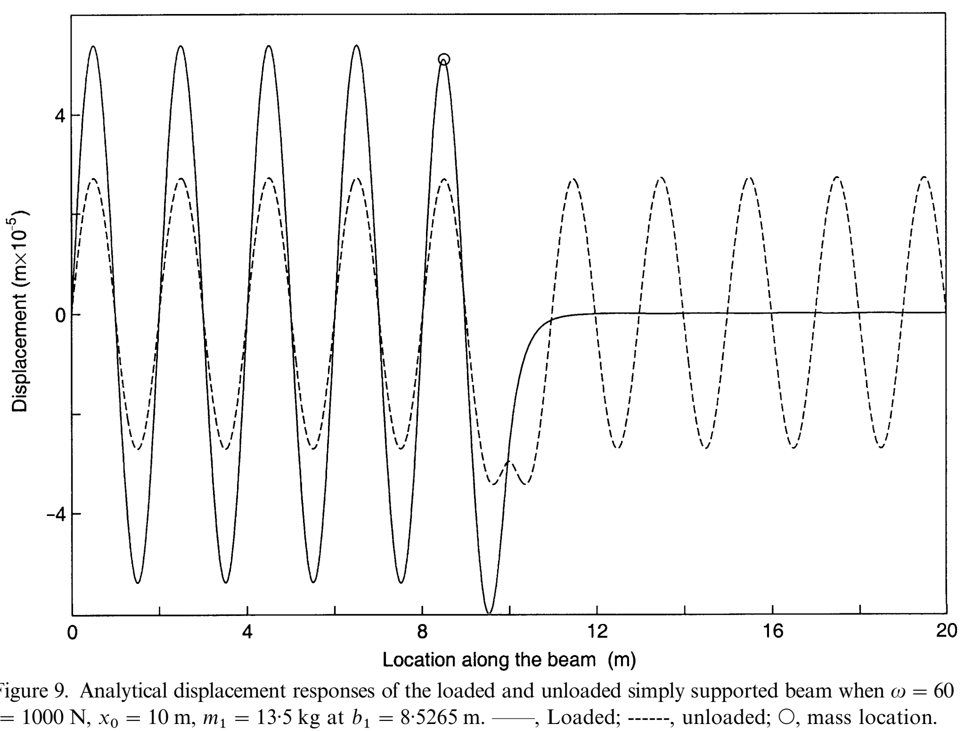

Figure 9. Analytical displacement responses of the loaded and unloaded simply supported beam when $\omega = 60$ Hz, $F_0 = 1000$ N, $x_0 = 10$ m, $m_1 = 13{\cdot}5$ kg at $b_1 = 8{\cdot}5265$ m. ——, Loaded; ------, unloaded; ○, mass location.

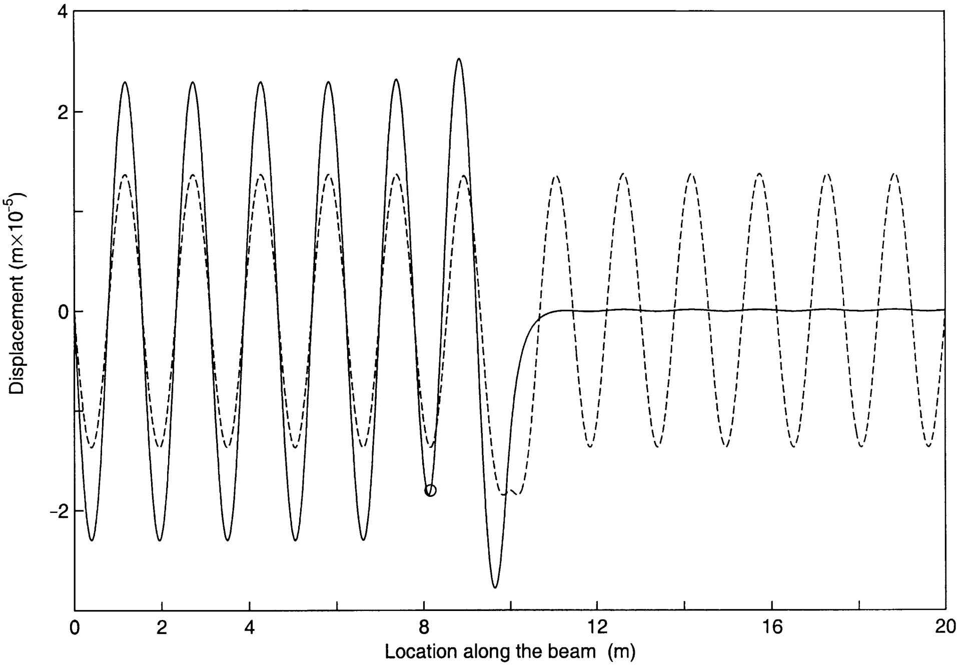

Figure 10. Analytical displacement responses of the loaded and unloaded simply supported beam when $\omega = 100$ Hz, $F_0 = 1000$ N, $x_0 = 10$ m, $m_1 = 55{\cdot}5$ kg at $b_1 = 8{\cdot}1587$ m. ——, Loaded; ------, unloaded; ○, mass location.

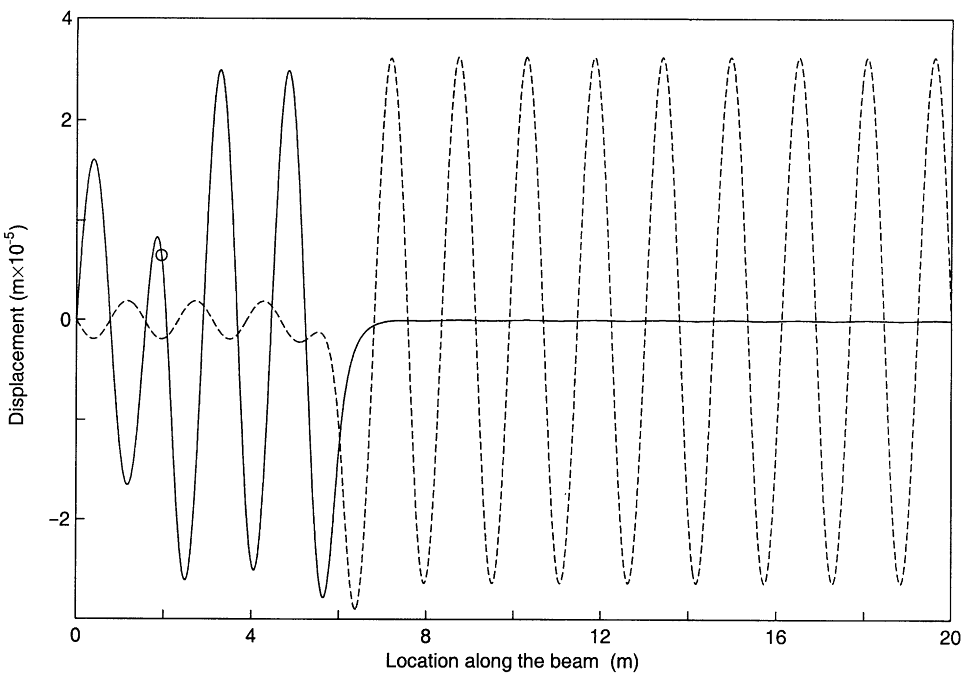

Figure 11. Analytical displacement responses of the loaded and unloaded simply supported beam when $\omega = 100$ Hz, $F_0 = 1000$ N, $x_0 = 6$ m, $m_1 = 299$ kg at $b_1 = 1{\cdot}9425$ m. ——, Loaded; ------, unloaded; ○, mass location.

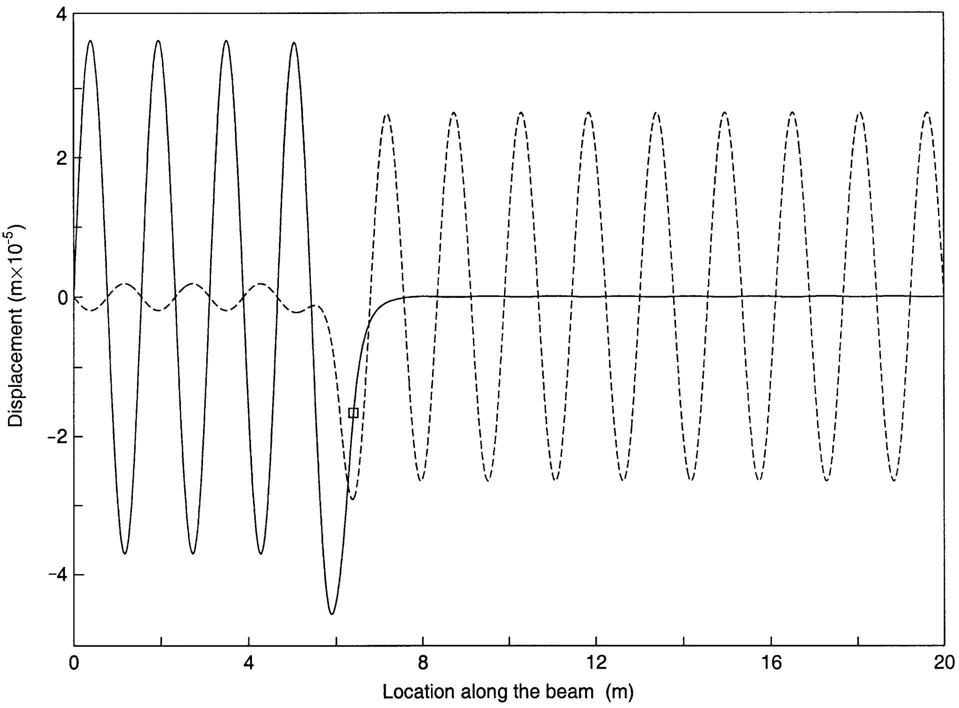

Figure 12. Analytical displacement responses of loaded and unloaded simply supported beam when $\omega = 100$ Hz, $F_0 = 1000$ N, $x_0 = 6$ m, $k = 68$ MN/m at $a_1 = 6{\cdot}4022$ m. ——, Loaded; ------, unloaded; □, spring location.

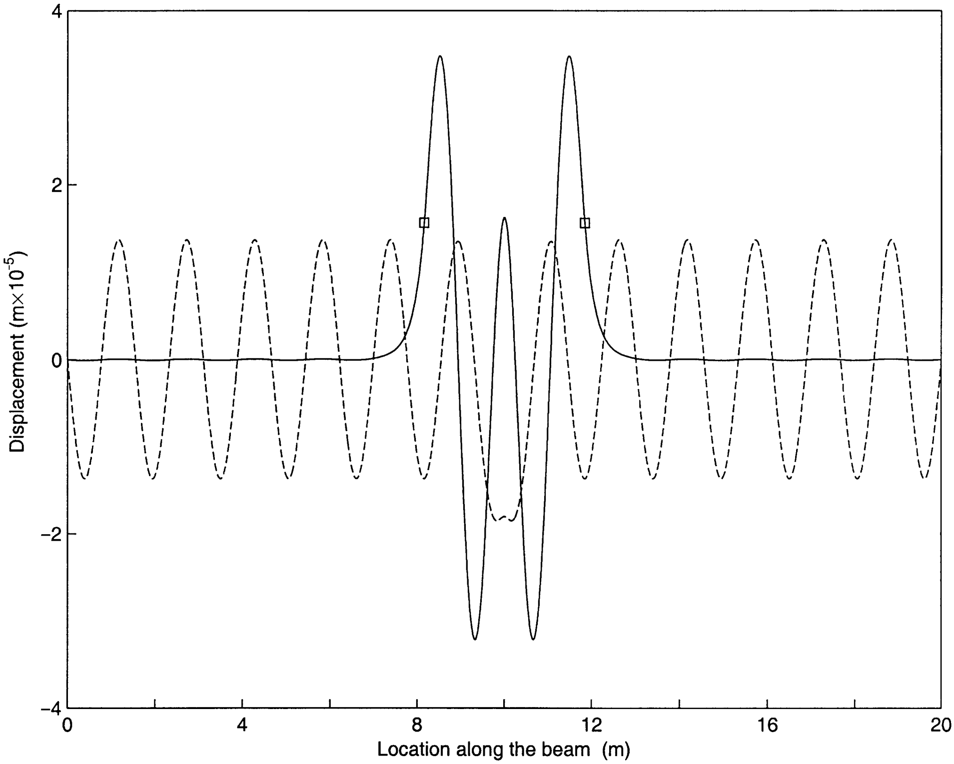

Figure 13. Analytical displacement responses of loaded and unloaded simply supported beam when $\omega = 100$ Hz, $F_0 = 1000$ N, $x_0 = 10$ m, $k_1 = k_2 = 80$ MN/m, $a_1 = 8{\cdot}1587$ m, $a_2 = 11{\cdot}8413$ m. ——, Loaded; ------, unloaded; □, spring location.

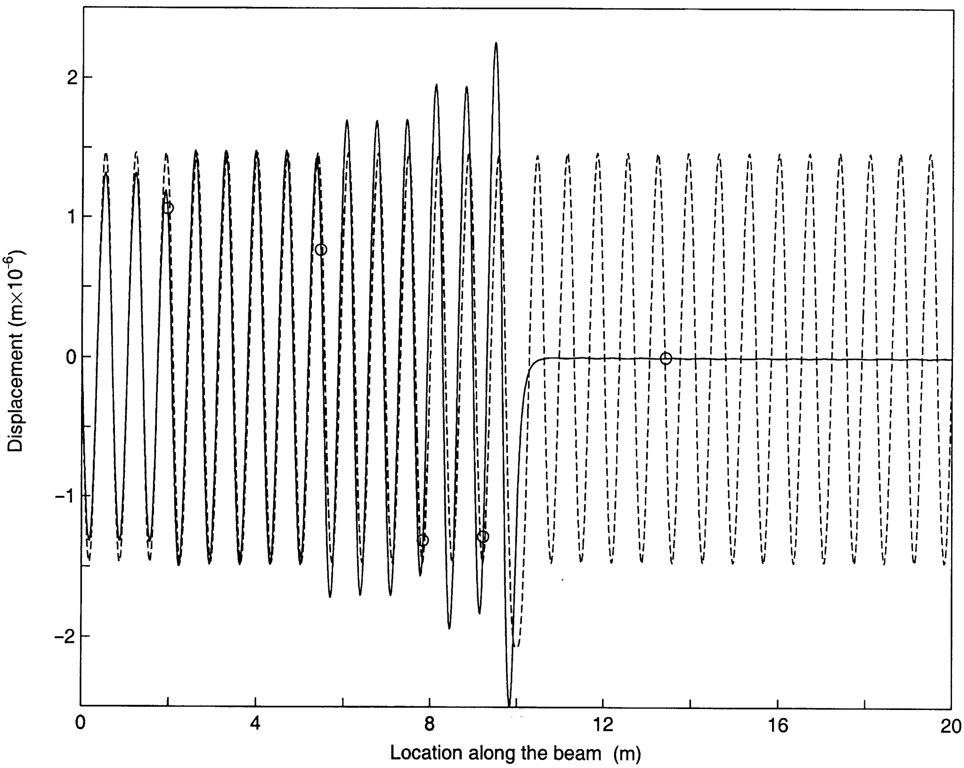

Figure 14. Analytical displacement responses of loaded and unloaded simply supported beam when $\omega = 500$ Hz, $F_0 = 1000$ N, $x_0 = 10$ m, mass set and locations from Figure 12 in reference [1]. ——, Loaded; ------, unloaded; o, mass location.

instead of a mass. In Figure 12, a spring of stiffness 68 MN/m is attached at $a_1 = 6{\cdot}4022$ m, which corresponds to $8{\cdot}75\lambda$ from the right end of the beam, and has a similar effect to a mass in controlling the propagation of vibration.

To suppress the transverse displacement responses on both sides of the beam, two springs with the same stiffness $k = 80$ MN/m are attached at $a_1 = 8{\cdot}1587$ m and $a_2 = 11{\cdot}8413$ m as shown in Figure 13. The excitation force of 1000 N acts at the mid-span of the beam. This figure was chosen for a good reason. Very often, one is interested in controlling the propagation of vibration in order to limit the vibration away from a source of mechanical disturbance.

Finally, Figure 14 shows the simulation results for the data of Figure 13 in reference [1]. Kellite and Cheng used five unequally spaced masses, each 15·6464 kg, to minimize the response on $x = 10$–20 m with a 500 Hz driving force at mid-span. Their optimal mass spacings, which were found by the principal axis optimization method, are found to be 1·9485, 5·51616, 7·8309, 9·2239 and 13·4211 m. In addition to a significant vibration reduction in comparison to their figure because of the truncation of modes in their analysis, inspection of Figure 14 shows that the fifth mass is redundant. Hence, one can get exactly the same vibration suppression with only four masses. Furthermore, one can use a single mass of value 42 kg located at any peak or trough in the left half of the beam and get exactly the same effects.

Figure 15 shows the dynamic response of a 4 m long cantilevered beam excited at its tip with an excitation force of 1000 N and 25 Hz excitation frequency. To suppress the vibration amplitude throughout the beam span, a spring with stiffness $K = 8$ MN/m is fixed

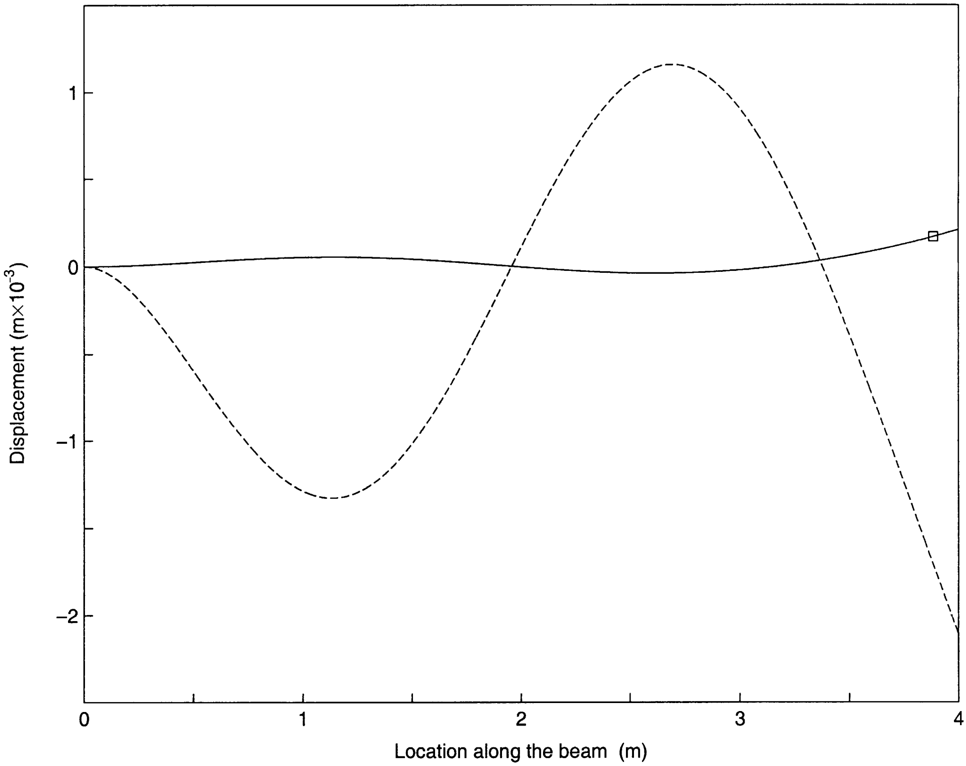

Figure 15. Analytical displacement responses of loaded and unloaded cantilevered beam when $L = 4$ m, $\omega = 25$ Hz, $F_0 = 1000$ N, $x_0 = 4$ m, $k_1 = 8$ MN/m, $a_1 = 3{\cdot}8851$ m. ——, Loaded; ------, unloaded, □, spring location.

at a distance $a_1 = 3{\cdot}8851$ m, which corresponds to $1{\cdot}25\lambda$. In comparison to the response of the unloaded beam, the displacement response of the spring-loaded beam indicates that a significant vibration reduction can be achieved.

5.1. OPTIMUM MASS RATIO

Consider again the simply supported beam from the previous section. The vibration confinement along the entire beam can be achieved near resonance conditions. Figure 16 depicts the displacement response of the simply supported beam at an excitation frequency of 25·5054 Hz (near resonance) with a single attached mass of 50 kg located at one of the peaks of the flexural wave of the unloaded beam ($b_1 = 5{\cdot}3849$ m). The mass ratio is 0.0123. The optimum mass ratio versus the excitation frequency, normalized with respect to the first natural frequency of the beam $\omega_1 = 0{\cdot}15094$ Hz, is shown in Figure 17. The optimum mass ratio is based on the minimum value of the attached mass required to achieve a significant vibration confinement along the beam at each external excitation frequency near resonance. Evidently, the force amplitude does not influence the suppressed displacement amplitude as revealed by Figure 18.

5.2. DUAL-EXCITATION FORCES

In order to control the vibration amplitude in the middle region of the beam the only way one can achieve this by imparting two identical excitation forces as shown in Figure 19. In

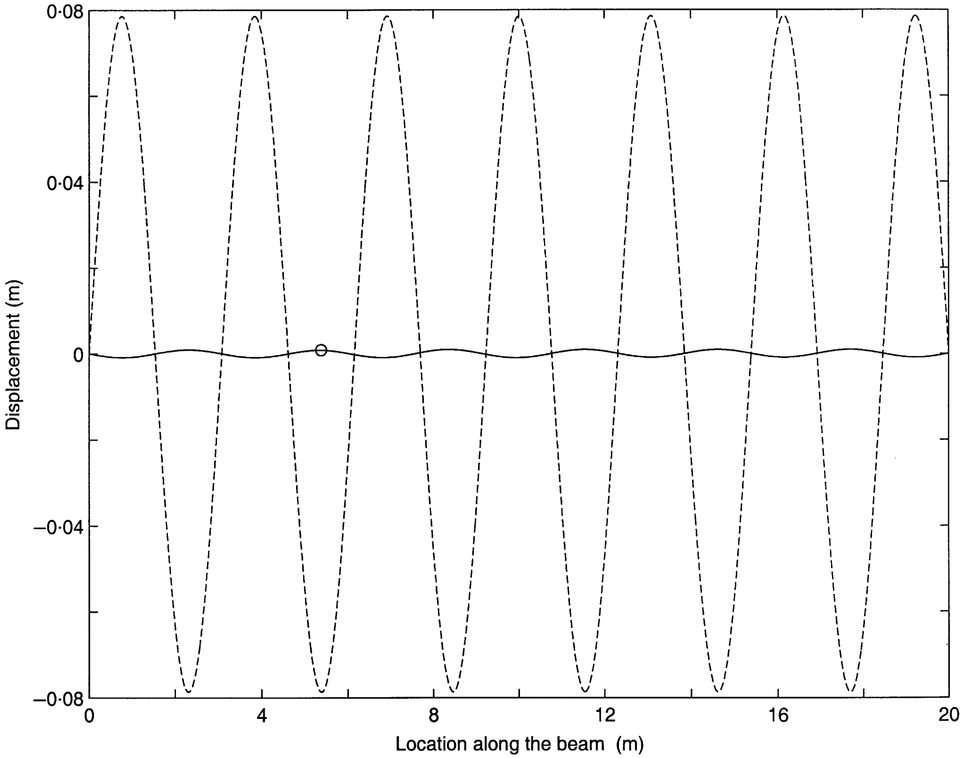

Figure 16. Analytical displacement responses of loaded and unloaded simply supported beam when $\omega = 25{\cdot}504$ Hz, $F_0 = 1000$ N, $x_0 = 10$ m, $m_1 = 50$ kg at $b_1 = 5{\cdot}3849$ m. ——, Loaded; ------, unloaded; ○, mass location.

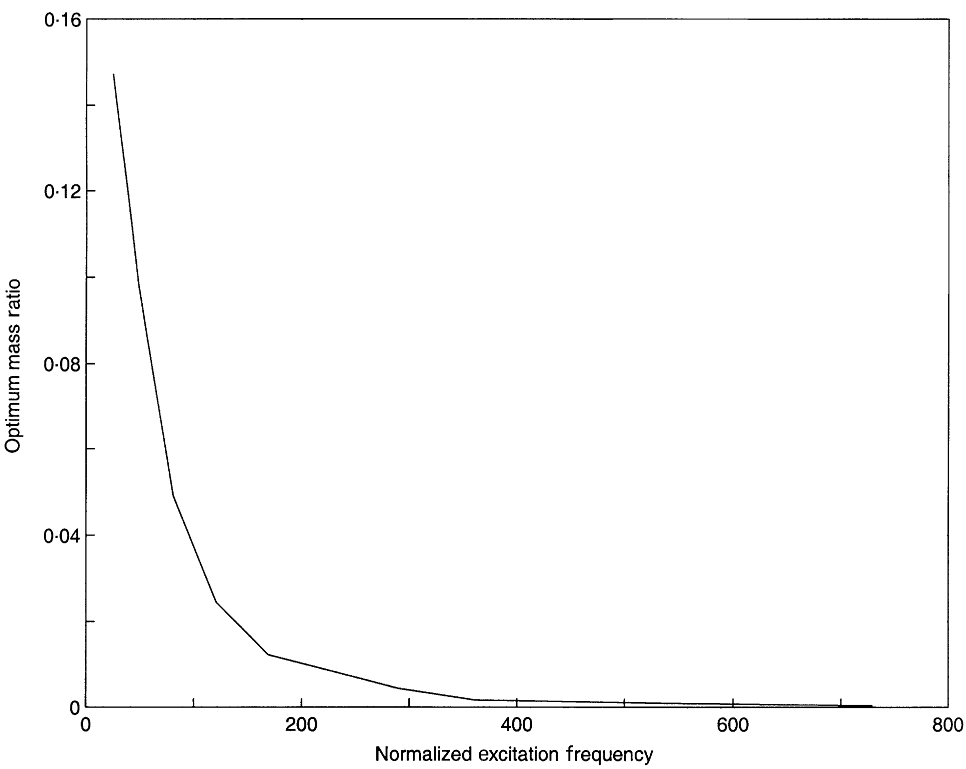

Figure 17. Minimum mass required for optimum vibration suppression versus input excitation frequency (at resonance).

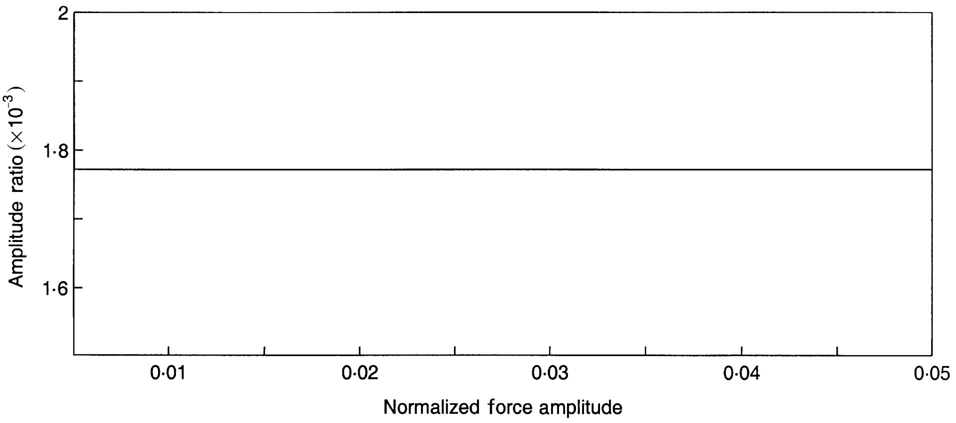

Figure 18. Suppressed vibration amplitude ratio versus excitation force when $\omega = 60$ Hz, $F_0 = 1000$ N, $x_0 = 10$ m, $m_1 = 13{\cdot}5$ kg at $b_1 = 8{\cdot}5265$ m, mass ratio $= 0{\cdot}0033$ (force normalized by $m\omega^2 L$).

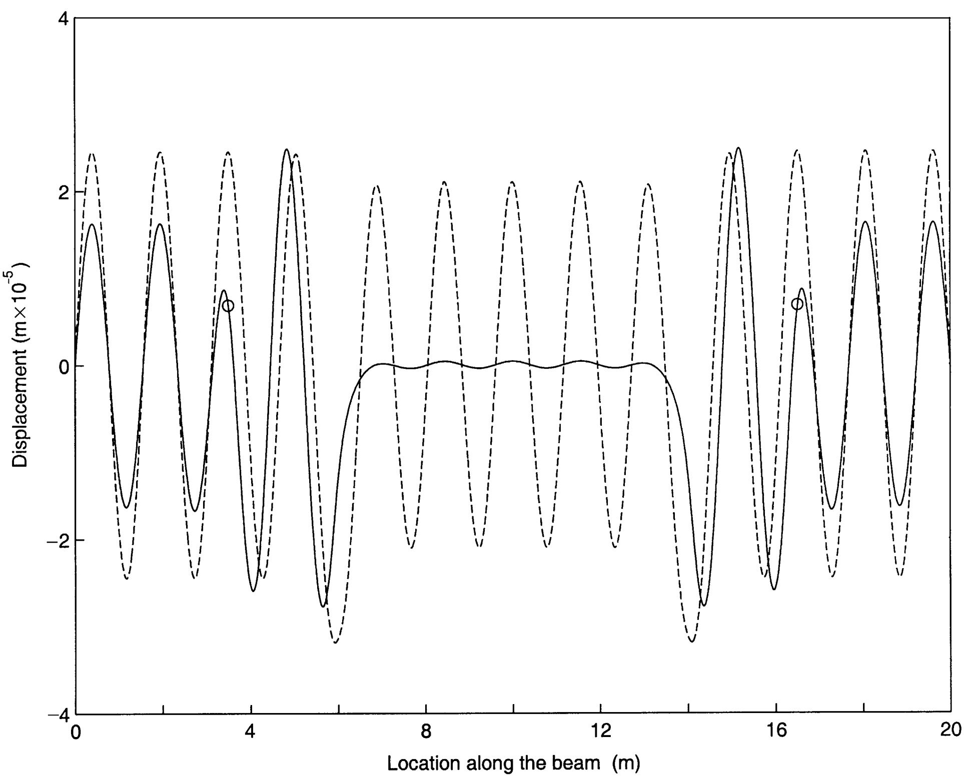

Figure 19. Dual excitations: vibration suppression within the interior region of the beam when $\omega = 100$ Hz, $m_1 = m_2 = 299$ kg, $b_1 = 3{\cdot}4966$ m, $b_2 = 16{\cdot}5034$ m. ——, Loaded; ------, unloaded; ○, mass location.

this figure the excitation forces act at $b_1 = 6$ m and $b_2 = 14$ m. The value of each force is 1000 N with a frequency of 100 Hz. The masses are 279 kg each and are attached at $b_1 = 3{\cdot}4966$ m and $b_2 = 16{\cdot}5034$ m. The distance between the forces can be used to control the segment length within which the vibration amplitude needs to be suppressed.

The purpose of the foregoing presentation was to display the versatility of the approach developed. Beams of various combinations of boundary conditions and Timoshenko-type beams can be treated in a similar manner. Simply, the Green function G (x, u) in the displacement expression is replaced by the proper one. Green functions for other complicated boundary conditions are tabulated in reference [9], while Green functions for Timoshenko-type beams are derived by Lueschen *et al.* [12].

6. CONCLUSION

In this investigation, a method based on the dynamic Green function has been proposed to determine the optimum values of masses and/or springs and their locations on a beam structure in order to suppress the vibration at an arbitrary location. The analytical displacement response for the case of a simply supported beam is verified experimentally using a laser measuring system and yielded reasonable results. As case studies, the vibrations of both simply supported and cantilevered beams can be controlled at an arbitrary location within the beam with a minimum value of attached point masses or springs. The optimum locations of the masses are found to be at peaks or troughs of the flexural wave of the unloaded beam forced response.

REFERENCES

1. R. F. KELTIE and C. C. CHENG 1995 *Journal of Sound and Vibration* **187**, 213–228. Vibration reduction of a mass-loaded beam.
2. Y. CHEN 1963 *Journal of Applied Mechanics* **30**, 310–311. On the vibration of beams and rods carrying concentrated masses.
3. P. A. LAURA, L. POMBO and E. SUSEMIHL 1974 *Journal of Sound and Vibration* **37**, 161–168. A note on the vibrations of a clamped–free beam with a mass at free end.
4. L. PARNELL and M. COBBLE 1997 *Journal of Sound and Vibration* **44**, 499–511. Lateral displacement of a vibrating cantilever beam with a concentrated mass.
5. M. GÜRGÖZE 1984 *Journal of Sound and Vibration* **96**, 461–468. A note on the vibrations of restrained beams and rods with point masses.
6. P. K. SARKAR 1996 *Journal of Sound and Vibration* **195**, 229–240. Approximate determination of the fundamental frequency of a cantilever beam with point masses and restraining springs.
7. M. GÜRGÖZE 1996 *International Journal of Mechanical Sciences* **12**, 1295–1306. On the eigenfrequencies of cantilevered beams carrying a tip mass and a spring mass in-span.
8. J. WU and T. LIN 1990 *Journal of Sound and Vibration* **136**, 201–213. Free vibration analysis of a cantilever beam with point masses by an analytical-and-numerical-combined method.
9. A. S. MOHAMED 1994 *International Journal of Solids and Structures* **31**, 257–268. Tables of Green's function for the theory of beam vibrations with general intermediate appendages.
10. G. ROACH 1981 *Greens Functions*. Cambridge: Cambridge University Press.
11. P. LUEG 1936 *U.S. Patent No.* 2043416. Process of silencing sound oscillations.
12. G. G. G. LUESCHEN, L. A. BERGMAN and D. M. MACFARLAND 1996 *Journal of Sound and Vibration* **196**, 93–102. Green's functions for uniform Timoshenko beams.